ADVANCED TECHNOLOGY DEMONSTRATION MOTOR: CASE-BONDED EXTRUDED DOUBLE-BASE GRAIN

Joseph Hong and Joseph Bellotte
BAE Systems, Ordnance Systems Inc.
4050 Peppers Ferry Road, Radford, Virginia

ABSTRACT

A critical disadvantage of cartridge-loaded rocket motors is the consumption of space by the structural hardware that immobilizes the grain. In an effort to eliminate this issue, BAE Systems Internal Research and Development (IRAD) at the Radford Army Ammunition Plant (RFAAP) has developed a motor that bonds directly to the motor wall thus removing the need for immobilizing hardware.

The bonding method requires an adhesive capable of withstanding nitroglycerin migration whilst maintaining the bond during loading, assembly, storage, transport, and firing of the motor. Laboratory, pilot-scale, and full-scale prototyping and experimentation was performed at RFAAP in addition to the development of loading and assembly methods for this new technology. Simulation of motor ballistics, fluid dynamics, thermal response, and structural integrity was also performed to anticipate the impact of the new design at various steps of motor manufacturing and testing. New hardware, data acquisition methods, sensor arrays, and analysis were developed for this design and incorporated into the test plan for 2018.

Simulation and analysis indicated an improvement in motor efficiency and performance, and preliminary static testing demonstrated a motor impulse increase of 12% over baseline. This program couples the rapid manufacturing effort typically found in production of cartridge-loaded rocket grains with a volumetric loading efficiency rivaling those found in cast-cure motors. Additional technologies are currently in development to further the capability and performance of cartridge-loaded/extruded double-base (EDB) rocket motors.

INTRODUCTION

BACKGROUND

IRAD began the Advanced Technology Demonstration Motor (ATDM) program in 2018. This program was conceived with the intent to develop technologies designed to improve the performance, capability, and efficiency of a rocket motor.

Building on prior work in materials research, development of the program began with the intent to case-bond the normally cartridge-loaded propellant grains produced at RFAAP. This effort would remove the spring immobilizer normally in place to prevent the grain from moving and replace it with additional propellant thus increasing motor impulse. To provide structural support, the grain would be bonded to the motor wall with adhesive.

SYSTEM ARCHITECTURE

IRAD looked to the historical performance of the 2.75” MK66 rocket motor used in the Hydra-70 missile system as a platform for developing the ATDM program. Being an R&D effort, a heavyweight motor assembly was desired for safety, analysis, feedback, and multiple-use purposes. IRAD referenced a motor design normally used for testing of new rocket development programs and modified the platform to allow for full-length bonding of a propellant grain to the motor wall. Additionally, the motor was altered to fit new forward attachments that accommodated the bonding effort. Figure 1 below shows an exploded view of the major components comprising the test motor for the ATDM program.

Index	Part
1	Nozzle
2	Aft Plate
3	Aft Collar
4	Motor Case
5	Propellant Grain
6	Forward Bulkhead

Figure 1: Motor Assembly Exploded View.

The nozzle assembly, including the nozzle, aft plate, and aft collar, remained unchanged from the existing heavyweight motor assembly used by R&D to test new motor designs. The nozzle assembly is designed as a failure point for the entire motor; in the event of over-pressurization, the bolts holding the nozzle to the motor case will fail and eject the nozzle rather than rupturing the heavy-walled tube.

As previously mentioned, the motor case remained largely unchanged from the existing heavyweight design, though ports used to measure forward and aft pressure had to be removed to allow for uniform bonding of the propellant grain. The case matches the 2.75” MK66 internal dimensions but has a substantially larger wall thickness to accommodate any issues that might arise from testing a new design. The inner surface finish was optimized for ideal bonding and the end threads are designed to interface with the existing test stand setup at RFAAP.

The propellant grain itself was also very similar in design to the standard MK90 propellant grain; only the outer diameter and overall length were increased. No alterations to the propellant composition (NOSIH-AA2) were made. This simplified production efforts at the Radford facility and also allowed for a direct comparison to the MK90 grain design if the ATDM propellant grain were loaded into the MK66 rocket motor. However, several components of the standard MK90 grain were removed from the motor. The ethyl cellulose (EC) wrap used for burn surface inhibition is not needed due to direct bonding to the motor wall. The EC motor end cap and forward end inhibitor are also not needed. Burn surface inhibition is, therefore, only needed at the aft-most end of the grain, so the aft end inhibitor was increased in outer diameter to protect the larger grain.

The forward bulkhead was modified to accommodate the new heavyweight design. A gas channel was drilled off-center through the component to provide a pressure reading at the head end. A forward face seal and rear threads were added to seal the forward end and connect the resonance rod, respectively. Forward threads were also tapped to provide a mounting/positioning point to load the bulkhead onto the motor assembly.

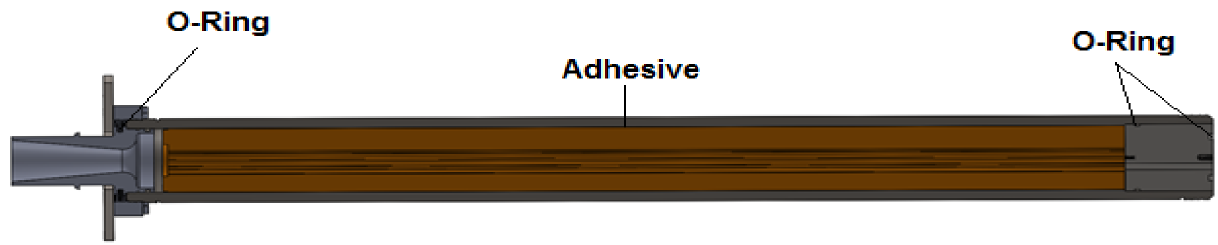

Figure 2: Motor Assembly.

Other components, including the forward thrust adapter and support hardware, were largely unchanged from the aforementioned R&D heavyweight motor assembly and had no positive or negative impact to motor performance.

METHODOLOGY

Prior research into adhesives and material interfaces conducted by BAE Systems involved laboratory, pilot-scale, and full-scale prototype testing to determine the integrity of a bond between rocket motor propellant and motor case materials. Adhesives were primarily selected based on their compatibility with energetic materials, ability to bond difficult surfaces, and low bond gap thickness.

Physical material failure occurs in shear, compression, tension, peel, or a combination of these modes. The expected failure of a propellant grain bonded in place is principally in shear during loading, assembly, storage, transport, and firing. Failure of the metal-propellant interface in these directions was tested initially at the laboratory scale in a modified lap-shear configuration. Lap shear testing followed ASTM Standard D3164 with tabs of propellant bonded between two metal substrates. Testing was performed at ambient, low, and high temperature conditions to imitate testing conducted with full-scale MK66 motors. Values were then compared to the forces expected on a static motor test to demonstrate the potential of the adhesive. The adhesive bonded strongly to AA-2 double-base propellant at all temperature conditions. Furthermore, the low bond gap thickness required to maintain bond integrity allowed for the greatest quantity of propellant to be loaded into a motor case.

An average of the results at ambient, high, and low temperatures are listed below in Figure 3. Low temperature testing of the lap shear configuration repeatedly indicated higher strengths than those between the mechanical testing machine grips and the metal substrates. As such, no formal failure strengths were recorded for low temperature testing. However, all values significantly exceeded the anticipated shear strength required to maintain propellant grain immobilization. Ambient and high temperature conditioned samples failed in a normal lap shear mode.

SIMULATION AND ANALYSIS

BALLISTIC ANALYSIS

Ballistic performance of the new grain was simulated with the commercially available solid rocket motor analysis software Solid Performance Program (SPP) ’12. The goal regarding grain design for the ATDM program was to volumetrically load as much propellant into the MK66 motor dimensions as possible. All simulation, therefore, followed a grain design that would best mate to the motor case walls while optimizing various rocket motor metrics.

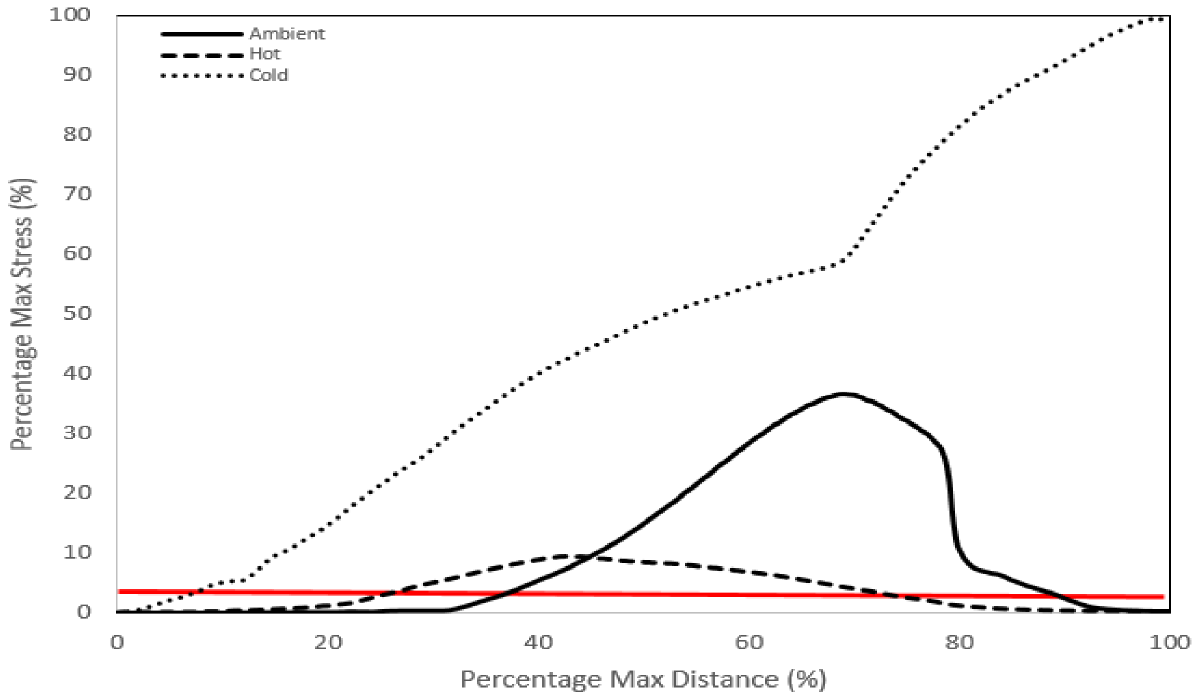

Figure 3: Summary of modified lap shear testing between AA-2 and stainless steel substrates at low (-50ºF), ambient (+77ºF), and high (+150ºF) temperatures. Minimum stress required to maintain grain immobilization (red line) based on surface area and motor pressure differential.

A quasi-one dimensional analysis was performed with SPP'12 to predict ballistic performance parameters. Thermochemistry and chemical composition properties dictate a characteristic velocity and expected burn rate for the propellant type and grain design. Interpretation of this data principally informs ballistic characteristics (action time, impulse, thrust levels) and any physical modifications needed (e.g. Mach relief cone).

The critical physical parameters (thrust, pressure) are regularly measured for motors tested at RFAAP. Profiles for such metrics are products of simulation with the SPP'12 software and are shown below in Figure 4. The plots show the increase in thrust and pressure solely due to the change in grain geometry. The profiles are largely in line with the standard profile generated by the MK66 rocket motor assembly indicating a slight increase in both thrust and pressure in addition to extending the burn time. Table 1 below shows additional increases in action time and impulse relative to the MK66 motor (see HW MK66). Analysis was performed at ambient and low temperature testing conditions (+77ºF, -50ºF). High temperature estimates (+150ºF) are shown below to demonstrate performance extremes for structural/physical analysis discussed later in this report.

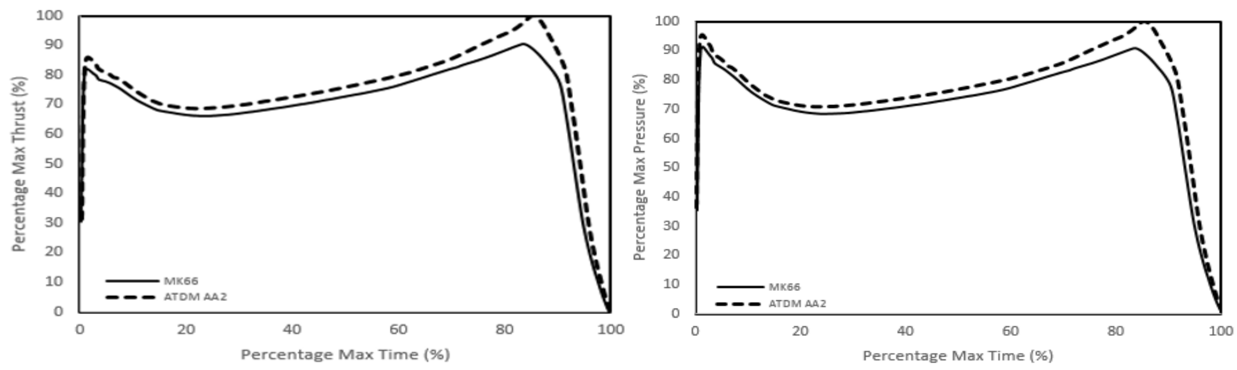

Figure 4: MK66 vs ATDM thrust (left) and pressure (right) curves at +150ºF.

COMPUTATIONAL FLUID DYNAMICS

Simulation of the fluid environment during burn of the ATDM grain was performed via computational fluid dynamics (CFD) software to determine various motor performance parameters. A three-dimensional, turbulent, Navier-Stokes analysis of the motor chamber and nozzle was performed at +150ºF under steady-state conditions.

CFD analysis of the motor exhaust determined pressure, temperature, and heat transfer boundaries. Fluid behavior is an important metric in determining structural and thermal effects on the motor and identifying potential problem areas prior to rocket testing. Internal forces and the differential pressure on the propellant grain during ignition and burn were important to the development of the ATDM program in particular due to the use of an adhesive as the source of immobilization. As previously mentioned, the MK90 assembly, used as a reference for this program, incorporates a compression spring to immobilize the grain in the motor case. To ensure the grain remained immobile during firing, the differential pressure between the forward and aft ends of this motor case would need to be less than the shear strength of the bond between the propellant and metal substrates. Laboratory testing of the bond interface was compared to CFD results and the metric for failure was shown previously in Figure 3.

Boundary conditions for the simulation are outlined in Table 2 below. Flow through the motor assembly remains subsonic until after the nozzle throat. A 1/16th symmetry model for the 8-point star propellant grain perforation was constructed of hexahedral mesh consisting of roughly 2×10^6 cells enclosed by a prismatic boundary layer. The fluid model itself was prepared with a static atmospheric pressure outlet and isothermal walls. Material temperatures were assumed static and erosive burning, burn augmentation rate, and igniter mass flow were not factored into the fluid model.

Boundary Conditions	
Regions	**Static Temperature (F)**
Aft End Inhibitor	335
Forward Inhibitor	
Wrap	
Salt Rod	
Case Wall	1000
Nozzle Wall	
Inlet	Mass Flux Inlet
Outlet	14.7 psi

Table 2: CFD model boundary conditions.

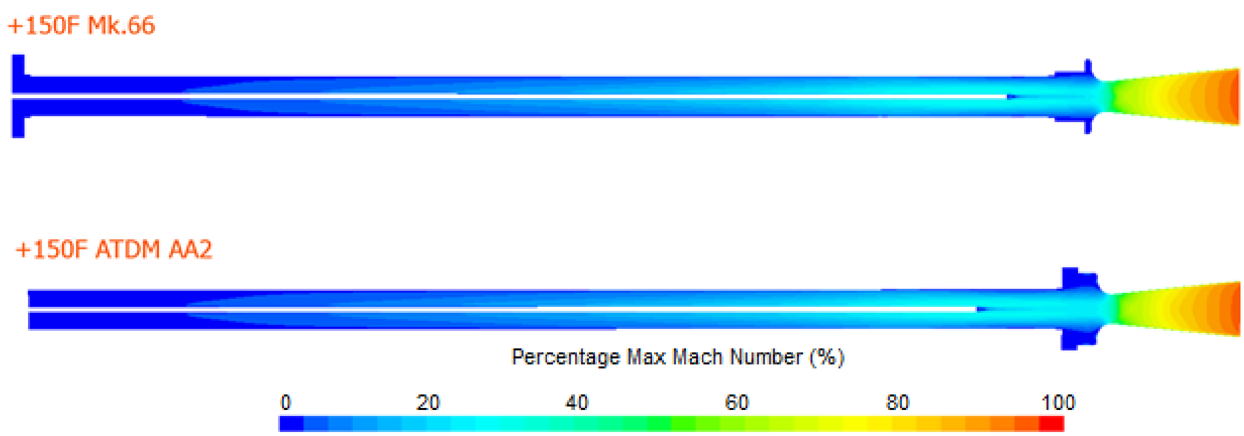

Figure 5: Mach Number flow chart comparison, MK90 vs ATDM profiles.

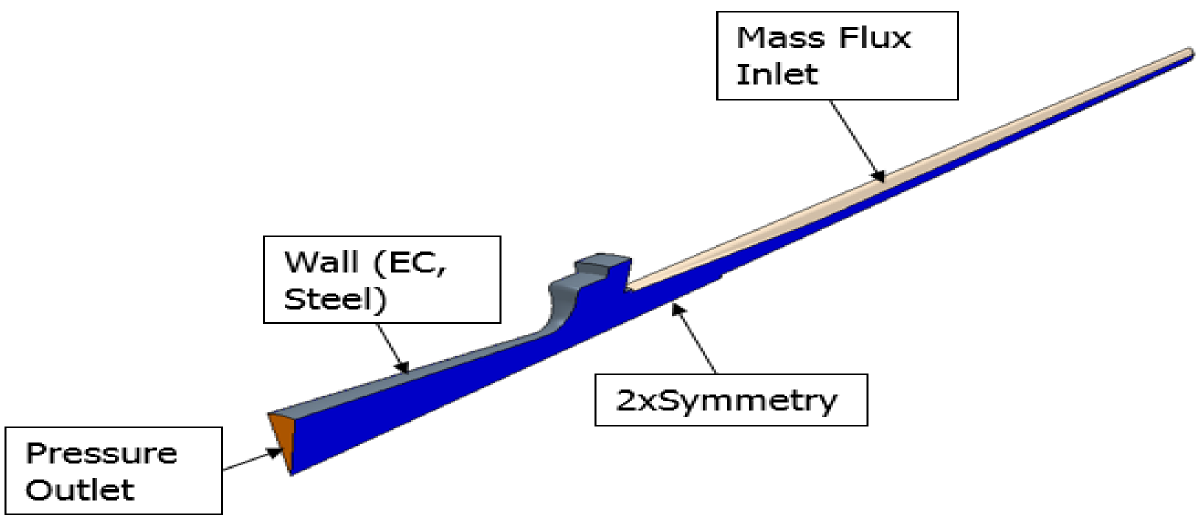

Figure 6: 1/16th symmetry model, ~2x10^{6} hexahedral mesh cells.

THERMAL ANALYSIS

The thermal environment during a static rocket fire is another important metric analyzed by FEA software. While IRAD did not anticipate a thermal failure of the stainless steel motor case during static testing, simulating the environment and comparing test results would help inform future designs should the motor case material be changed or the dimensions altered. CEA thermochemical equilibrium code helped to calculate thermodynamic and transport properties for the expected fluid-exhaust products stemming from an AA-2 propellant burn. Assumptions regarding erosive burning and static material characteristics largely refute any changes to the thermal environment. While these parameters make simulation easier, the physical model is more accurately informed by the temperature-sensitive changes to specific heat, thermal conductivity, and viscosity.

STRUCTURAL ANALYSIS

Static structural analysis was performed to determine the integrity of the newly designed heavyweight case. While the ATDM program based its motor case design off an approved, existing case for testing, the change in grain geometry mandated a review of hardware response. Additionally, repeated use of this motor assembly was anticipated and modal analysis of the structural integrity was desired.

The primary motor components were constructed of 300 Series Stainless Steel which provided substantial structural integrity to the design. Static analysis was performed under worst-case-scenario conditions which assumed a catastrophic failure of the case-bonding effort. This exposes the outer burn surface which substantially increases the motor internal pressure during firing. However, failure points were explicitly designed into the nozzle attachment hardware so in the event of an over pressurization event, the nozzle would be expelled rather than rupture the case.

Internal motor pressure was simulated to immediately rise to the maximum expected pressure and remain constant for the anticipated burn duration. While it was not expected that the propellant burn would cause a constant high pressure burn through the expected burn time, this mode, coupled with the pressure determined from catastrophic failure, helped ease concerns in the event of a worst-case-scenario.

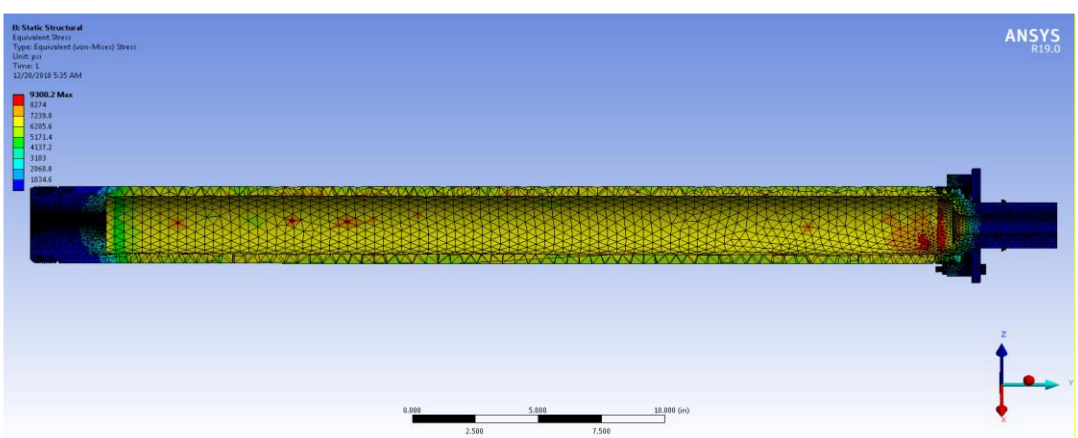

Figure 8: Total simulated deformation of ATDM heavyweight motor case, catastrophic event showing internal stress.

Figure 8 above shows the internal stress and factor of safety metrics for the motor under internal pressures measured from CFD analysis. Design integrity is maintained throughout the motor profile relative to the standard yield stress of 316 stainless steel (~25 ksi) and the factor of safety exceeds 3.0 at all surfaces.

TESTING

Motors were assembled by securing the forward bulkhead into the motor case and pouring a pre-measured volume of adhesive into the tube. The propellant grain followed the adhesive into the case and flowed up and around the propellant grain due to a seal at one end of the perforation. The grain was stabilized and centered in the tube until a working cure of the adhesive was achieved. Additional and supporting hardware were added to the assembly once a full cure was realized. Motors were maintained at 77ºF until static firing.

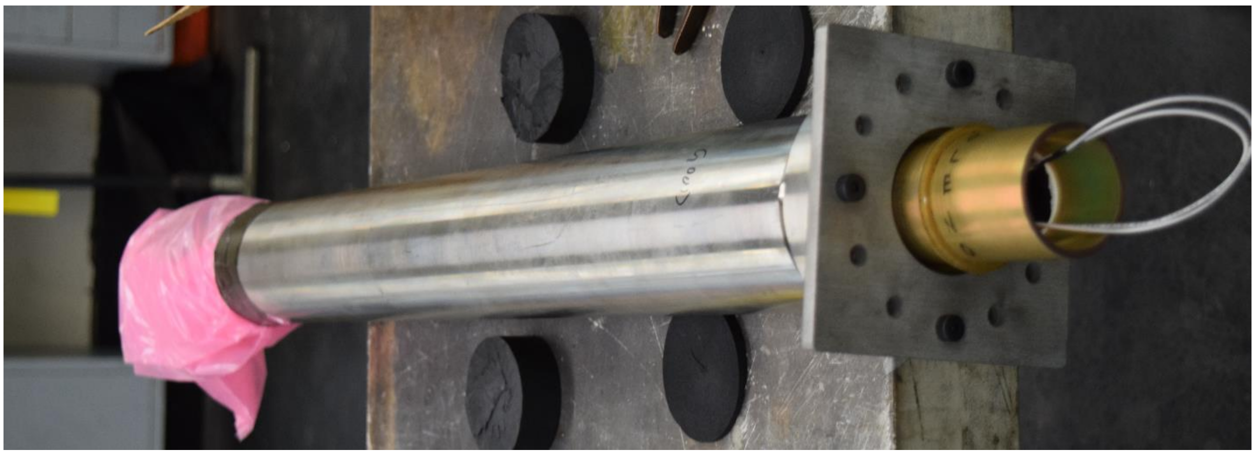

Image 1: Assembled ATDM heavyweight motor case.

An open air test of the motor assembly was conducted at the static test facility at RFAAP. Forward chamber pressure, thrust, and high and normal speed video were recorded.

Image 2: Snapshot of high-speed footage at ignition (left), mid-burn (middle), and end-burn (right) timeframes.

RESULTS

Both motors tested ignited properly and maintained structural integrity throughout the burn. Results show predictions for the forward motor pressure, thrust, and motor impulse were largely accurate and indicate an increase in motor impulse of over 12%.

Post-firing analysis was performed on all associated hardware. Specifically, the motor case internal surface was photographed and analyzed to determine if any significantly negative impact could be identified. Image 3 below shows a thin layer of partially charred adhesive remaining on the motor surface at both ends of each motor. Prior to testing, some charring was expected of the cured adhesive. However, no evidence of flaking or fracture of the adhesive was present. The remaining adhesive appeared to be largely uniform in dimension (i.e. no fracture or cracking due to exposure to the exhaust gases/flame) and no indication the motor walls themselves had been structurally or thermally compromised. Burn-back of the propellant web appears to have been largely uniform for both test motors as the 8-star pattern can be seen in Image 3. Test pieces of EPDM insulation placed at the aft-most ends of each motor case were largely consumed and showed heavy charring (see ‘right’ of Image 3 below).

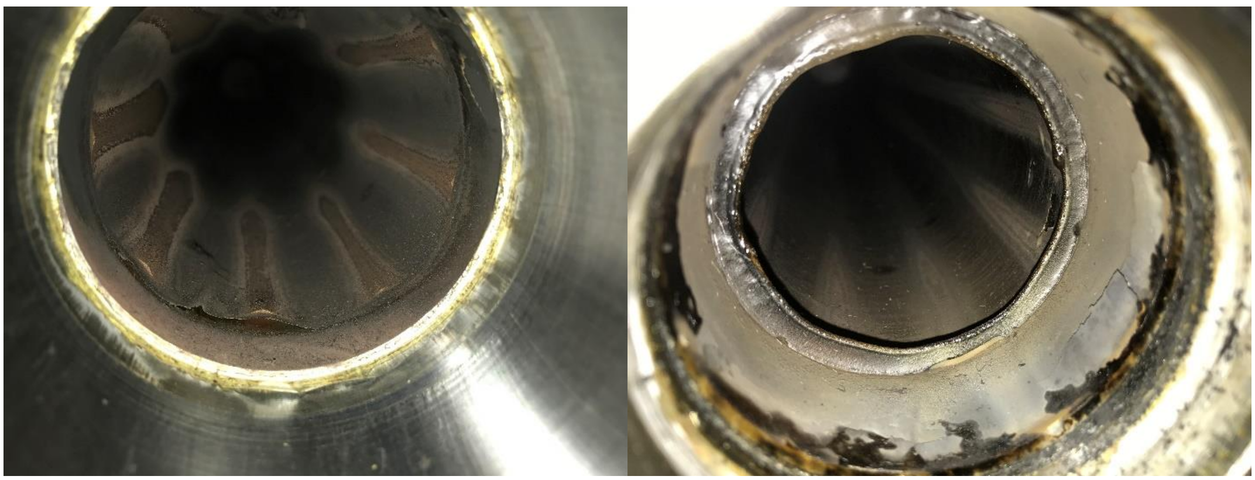

Image 3: Forward (left) and aft (right) images post-firing of ATDM static test.

The thrust and pressure profiles in Figure 9 below show the static test results were largely in line with predictions for both parameters and resulted in an increase to motor impulse of roughly 12% over baseline. Instability towards the end of the burn was attributed to the unaltered resonance rod that was copied from the standard MK66 platform. Motor disassembly during post-test analysis showed the resonance rods had been largely consumed during testing. Both motor rods had roughly 9.5 inches in length remaining from an initial length of thirty (30) inches.

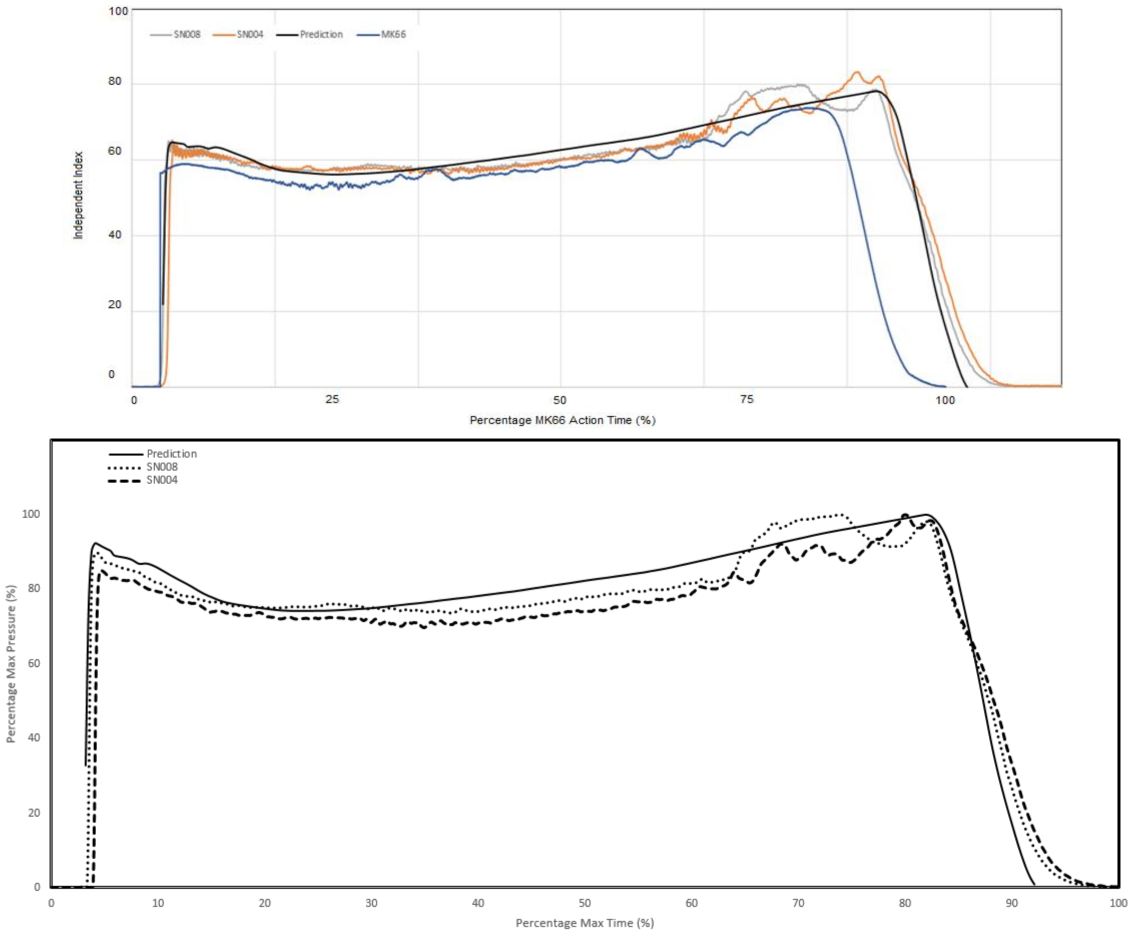

Figure 9: Final thrust (top) and head-end pressure (bottom) curves for predicted and actual motor performance.

CONCLUSIONS AND FUTURE WORK

Development of the ATDM program successfully tested an assembly for case-bonding a cartridge-loaded rocket motor grain. Adhesive intended to keep the propellant grain immobile before and during static test firing proved its potential and the motor matched expectations for all critical performance parameters. The 12% increase in motor impulse relative to baseline demonstrates the capability of this assembly and sets a platform for future development. Testing also demonstrated the capability of the motor as designed and general integrity of the system to test rocket propellant grains. Additional modifications to the igniter design, data acquisition method, and propellant machining were also confirmed successful in the test of this system.

Current efforts are focused on additional sensor arrays for motor feedback, improving loading and assembly methodologies for greater consistency, modification to motor hardware to relieve burn instability, and motor performance at conditioned temperatures. Additionally, the ATDM program plans to incorporate advances in technology pertaining to higher density energetics, lightweight materials, and improved flow dynamics to further demonstrate rocket motor performance.